# Continuous-wave laser oscillation at 1.3 $\mu$m in Nd:YAG proton-implanted planar waveguides

M. Domenech
*Departamento de Física de Materiales, C-IV, Universidad Autónoma de Madrid, 28049-Madrid, Spain*

G. V. Vázquez
*Centro de Investigaciones en Óptica, Loma del Bosque 115, Lomas del Campestre, 37150, León, Guanajuato, México*

E. Flores-Romero
*Departamento de Óptica, CICESE, km 107 Carr. Tijuana-Ensenada, Ensenada, B.C. 22860, Mexico*

E. Cantelar and G. Lifante[a)]
*Departamento de Física de Materiales, C-IV, Universidad Autónoma de Madrid, 28049-Madrid, Spain*

(Received 4 January 2005; accepted 22 February 2005; published online 6 April 2005)

This work reports continuous laser oscillation around 1.3 $\mu$m at room temperature in Nd:YAG planar waveguides fabricated by MeV proton implantation. The performance of the waveguide lasers fabricated with different implantation parameters has been studied in terms of the threshold pump powers and slope efficiencies. These results have been compared with those obtained in Nd:YAG waveguide lasers operating at a wavelength of 1.06 $\mu$m, taking into account the different emission cross-sectional values of the ${}^4F_{3/2} \rightarrow {}^4I_{11/2}$ and ${}^4F_{3/2} \rightarrow {}^4I_{13/2}$ transitions. © *2005 American Institute of Physics*. [DOI: 10.1063/1.1899240]

The development of compact and efficient solid state lasers is becoming an important matter in the field of integrated optics. The waveguide configuration is necessary in applications such as optics communications and information technology due to its size and compatibility with semiconductor lasers and fiber optic technology.[1] Optical waveguides doped with rare-earth ions can be used for the development of miniaturized lasers and amplifiers providing high slope efficiency and low pump thresholds.

Ion beam implantation has proved to be an effective technique to fabricate optical waveguides in more than 60 materials.[2] The damage caused by nuclear collisions during the implantation process reduces the physical density of the crystal, which results in a reduction of the refractive index. The low-density buried layer that is produced at the end of the ion track acts as an "optical barrier" that has a lower refractive index than the substrate.[3] Thus, the region between this barrier and the surface is surrounded by regions of lower refractive index and can act as a waveguide. Nd:YAG was the first material in which such a structure was formed by ion implantation and where the suitability of this technique to fabricate waveguide lasers was demonstrated.[4]

Laser oscillation in the cw regime in proton and carbon implanted Nd:YAG waveguides at 1064 nm has been recently reported, showing low pump thresholds and high stability.[5] This work presents laser emission at 1338 nm obtained from proton-implanted waveguides, which corresponds to the second telecommunication window in silica optical fibers. Characteristics such as pump power thresholds and laser efficiencies are reported, and these data are compared with the performance of Nd:YAG waveguide lasers operating at 1.06 $\mu$m.

Two planar waveguides were fabricated by proton implantation in a 9SDH-2 Pelletron Accelerator using protons of several energies and different total doses.[6] Waveguide #1 was implanted with energies from 1.25 to 1 MeV at a total dose of $6\times10^6$ ions/cm$^2$, while for waveguide #2 the implanted energies were from 1.15 to 1 MeV at an angle of 30° and a final dose of $5\times10^{16}$ ions/cm$^2$. When a waveguide is formed by ion implantation, color centers are generated during the process, which would imply absorption losses in the waveguide.[2] Therefore, an annealing step is necessary in order to reduce these losses. In the present work both Nd:YAG waveguides were introduced during half an hour in an open furnace operating at 400 °C.

To ascertain in which extent the spectroscopic properties of the neodymium ions are affected by the ion implantation process, a cw Ti:sapphire laser, with a tuning range between 750–850 nm, was used as excitation source and launched into the planar waveguides by means of a $\times10$ microscope objective. The output light was collected through a $\times20$ microscope objective, directed to the entrance slit of a monochromator (ARC SpectraPro 500-i) and detected by using an InGaAs photodiode. Cw laser operation was performed by coupling the waveguides to a resonant cavity formed by butting two dielectric mirrors to the polished end faces of the planar waveguides. A mirror of reflectivity $>$99.8% at 1338 nm and a transmittance $>$99% at 822 nm was placed in the rear face, while on the output face a mirror of reflectivities 95% at 1338 nm and $>$90% at 822 nm was used. The pump beam from the Ti:sapphire source was coupled again into the waveguide by the end-fire coupling technique. The pump power as well as the laser output power from the waveguide were measured by a Spectra Physics Model 407A power meter and a germanium photodiode (Thorlabs), respectively.

The waveguides were optically characterized by means of the standard *m*-line technique and their refractive index profiles at $\lambda=633$ nm were constructed by a multilayer approximation.[6,7] It was found that waveguide #1 presents an optical barrier height (decrease in refractive index relative to

[a)]Electronic mail: gines.lifante@uam.es

 

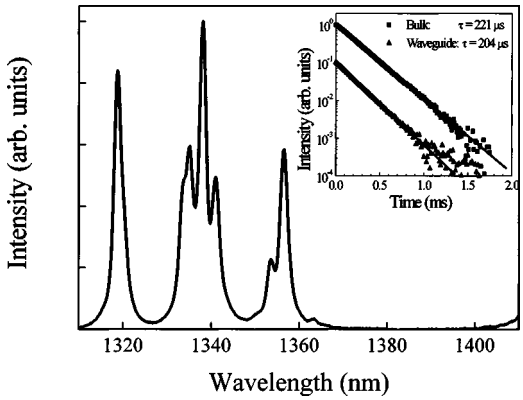


FIG. 1. Partial spontaneous emission spectrum of the $Nd^{3+}$ ions from a proton-implanted Nd:YAG waveguide after excitation at 822 nm. Inset shows the luminescence decays at $\lambda_{emi}=1.34$ $\mu$m corresponding to bulk sample (squares) and ion-implanted waveguide (triangles).

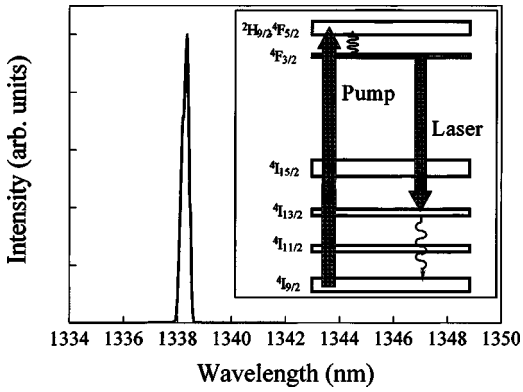


FIG. 2. Laser spectrum of the ion implanted Nd:YAG waveguide laser after 822 nm pump. Inset presents the partial level diagram of the $Nd^{3+}$ ions involved in the laser operation.

the substrate) of approximately 0.98% with a depth of 9.5 $\mu$m; on the other hand, the barrier height induced by the ion implantation process for waveguide #2 is ~0.6% and is situated at 8 $\mu$m beneath the surface. These measurements allow one to confirm that the fundamental mode is confined at 1.3 $\mu$m for both waveguides.

The spontaneous emission spectra of the $Nd^{3+}$ ions in YAG corresponding to the ${}^4F_{3/2}\rightarrow{}^4I_{13/2}$ transition under excitation at 822 nm for waveguide #1 is shown in Fig. 1, being coincident with that previously reported in bulk-doped Nd:YAG.[6] Although the bands situated around 1.32, 1.34, and 1.36 $\mu$m have emission peaks with similar emission cross sections, the most intense centered at 1338.5 nm has the highest probability for stimulated optical amplification. The inset of Fig. 1 shows the fluorescence lifetime of the ${}^4F_{3/2}$ metastable level measured in the bulk and in the waveguide, obtained by modulating the excitation beam with a mechanical chopper. The signal, averaged and recorded with a digital oscilloscope, shows single-exponential decays with lifetimes of 204 $\mu$s for the waveguide and 221 $\mu$s for the bulk. As rare-earth ions are fairly insensitive to the surroundings, we do not expect changes in the radiative characteristics of the $Nd^{3+}$, while in general, the nonradiative properties are much more sensitive to the ionic environment, and severe effects have been observed in some materials.[8] Therefore, the shortening of the lifetime could possibly be attributed to an increase in the nonradiative probabilities, that is, a slight deformation of the original substrate due to the implantation process.

After excitation to the ${}^4F_{5/2}$ manifold, the $Nd^{3+}$ ions relax mainly via nonradiative decay to the ${}^4F_{3/2}$ metastable level, where radiative and nonradiative transitions take place to the lower-lying levels (${}^4I_{15/2}$, ${}^4I_{13/2}$, ${}^4I_{11/2}$, ${}^4I_{9/2}$). If stimulated emission occurs, the ${}^4F_{3/2}\rightarrow{}^4I_{13/2}$ transition dominates over all other de-excitation processes, which become short-circuited (see inset in Fig. 2) and an intense infrared emission can be observed. As is shown in Fig. 2, the active waveguide operating in free running mode lased in cw manner at 1338.3 nm, with a measured full width at half-maximum of 0.5 nm, this experimental value being limited by the resolution of the monochromator (~0.2 nm).

Once the laser was emitting in continuous regime at room temperature, the most important laser features, that is, the pump power at threshold and the slope efficiency, of the implanted Nd:YAG planar waveguides, were measured. In Fig. 3 the laser output power versus launched pump power when the Ti:sapphire laser was tuned at 822 nm is presented for both waveguide lasers. The launched pump power needed to reach laser action for waveguide #1 (Fig. 3, squares) is 62 mW and the slope efficiency is around 13%, while for waveguide #2 (Fig. 3, circles) the power threshold is 91 mW and the efficiency around 9%. For the available pump powers, the proton-implanted planar waveguides (#1 and #2) can emit up to 3.5 and 4.5 mW at $\lambda=1338.3$ nm in a continuous wave manner, respectively. It can be clearly observed that the deepest planar waveguide (#1) with the highest optical barrier has the lowest power threshold, probably due to the fact that the fundamental mode is better confined in the structure, while the slope efficiencies are very similar for both waveguides.

The pump power threshold depends directly on the effective area of the fundamental mode and on the emission cross section by:[9,10]

$$P_{\text{th}}=\frac{h\nu_P}{\eta\sigma_e\tau}\frac{\delta}{2}A_{\text{eff}}, \tag{1}$$

where $\nu_P$ is the pump frequency, $\sigma_e$ is the stimulated emission cross section, $\tau=204$ $\mu$s is the fluorescence lifetime, $\eta$ is the fraction of absorbed photons that contribute to the population of the ${}^4F_{3/2}$ metastable state ($\eta=1$), $A_{\text{eff}}$ is the effective pump area, and $\delta$ the round-trip cavity exponential factor, which depends on the scattering losses ($\alpha$), the cavity

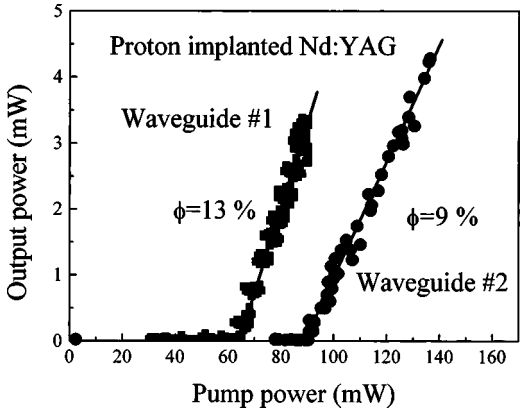


FIG. 3. Laser output characteristics of the free-running proton implanted waveguide lasers #1 and #2 operating at 1338.5 nm at room temperature.

length ($l$), and the input ($R_1$) and output ($R_2$) mirror reflectivities by $\delta=2\alpha l-\ln(R_1R_2)$. Equation (1) allows to compare the results here reported with those obtained at an emission wavelength of 1064 nm, which exhibit the highest emission cross section. Previous measurements for the ${}^4F_{3/2}\rightarrow{}^4I_{11/2}$ transition of the Nd:YAG proton-implanted waveguides revealed that for waveguide #1 the pump power needed to reach laser oscillation was 11 mW (see Ref. 10) and 23 mW for waveguide #2. Considering that $\sigma_e=3.1\times10^{-19}$ cm$^2$ (see Ref. 11) for the ${}^4F_{3/2}\rightarrow{}^4I_{11/2}$ transition and $\sigma_e=8\times10^{-20}$ cm$^2$ (see Ref. 12) for the ${}^4F_{3/2}\rightarrow{}^4I_{13/2}$ transition, this gives that the pump power threshold should be nearly four times higher for the laser emission at around 1.3 $\mu$m than for the 1.06 $\mu$m emission. Experimentally, we have found that the ratio of the thresholds needed to reach laser oscillation for the ${}^4F_{3/2}\rightarrow{}^4I_{13/2}$ and for the ${}^4F_{3/2}\rightarrow{}^4I_{11/2}$ transitions are 5.6 and 4.0 for waveguides #1 and #2, respectively, in close agreement with the theoretical estimations.

In conclusion, Nd:YAG waveguide lasers fabricated by the proton implantation technique with different fabrication parameters operating at 1338.5 nm were demonstrated. The spectroscopic characterization of the neodymium ions in this host as well as the laser characteristics have been reported, showing the waveguide #1 a threshold of 62 mW with a slope efficiency of around 13% and the waveguide #2 a threshold of 92 mW and $\phi=9\%$. The pump power laser thresholds have been compared with the data on laser oscillation around 1064 nm in terms of the emission cross section of the different transitions.

This work has been partially supported by Ministerio de Educación (Spain) under Project No. TIC2002-00147, and CONACYT (Mexico) under Project Nos. G0010-E and F036-E9109.

[1] D. Barbier and R. L. Hyde, in *Integrated Optical Circuits and Components: Design and Applications*, edited by E. J. Murphy (Marcel Dekker, New York, 1999).
[2] P. D. Townsend, P. J. Chandler, and L. Zhang, *Optical Effects of Ion Implantation* (Cambridge University Press, Cambridge, UK, 1994).
[3] P. D. Townsend, Nucl. Instrum. Methods Phys. Res. B **46**, 18 (1990).
[4] L. Zhang, P. J. Chandler, P. D. Townsend, S. J. Field, D. C. Hanna, D. P. Shepherd, and A. C. Tropper, J. Appl. Phys. **69**, 3440 (1991).
[5] M. Domenech, G. V. Vázquez, E. Cantelar, and G. Lifante, Appl. Phys. Lett. **83**, 4110 (2003)
[6] G. V. Vázquez, J. Rickards, H. Márquez, G. Lifante, E. Cantelar, and M. Domenech, Opt. Commun. **218**, 141 (2003).
[7] G. Lifante, *Integrated Photonics: Fundamentals* (Wiley & Sons, Chichester, UK, 2003).
[8] G. A. Torchia, G. V. Vázquez, E. Cantelar, G. Lifante, and F. Cussó, J. Phys. IV, (in press).
[9] E. Lallier, J. P. Pocholle, M. Papuchon, M. P. De Micheli, M. J. Li, Q. He, D. B. Ostrowsky, C. Grezes-Besset, and E. Pelletier, IEEE J. Quantum Electron. **27**, 618 (1991).
[10] M. Domenech, Doctoral thesis, Universidad Autónoma de Madrid, 2004.
[11] S. J. Field, D. C. Hanna, D. P. Shepherd, A. C. Tropper, P. J. Chandler, P. D. Townsend, and L. Zhang, IEEE J. Quantum Electron. **27**, 428 (1991).
[12] J. Lu, M. Prabhu, J. Song, C. Li, J. Xu, K. Ueda, A. A. Kaminskii, H. Yagi, and T. Yanagitani, Appl. Phys. B: Lasers Opt. **71**, 469 (2000).